J|A|C|S COMMUNICATIONS

Published on Web 12/14/2010

Importance of Oxygen in the Metal-Free Catalytic Growth of Single-Walled Carbon Nanotubes from SiO_x by a Vapor−Solid−Solid Mechanism

Bilu Liu,[†,§] Dai-Ming Tang,[†,§] Chenghua Sun,[‡] Chang Liu,[†] Wencai Ren,*[,†] Feng Li,[†] Wan-Jing Yu,[†] Li-Chang Yin,[†] Lili Zhang,[†] Chuanbin Jiang,[†] and Hui-Ming Cheng*[,†]

Shenyang National Laboratory for Materials Science, Institute of Metal Research, Chinese Academy of Sciences, Shenyang 110016, People's Republic of China, and ARC Center of Excellence for Functional Nanomaterials, School of Engineering, and Center for Computational Molecular Science, Australian Institute for Bioengineering and Nanotechnology, The University of Queensland, QLD 4072, Australia

Received September 1, 2010; E-mail: wcren@imr.ac.cn; cheng@imr.ac.cn

Abstract: To understand in-depth the nature of the catalyst and the growth mechanism of single-walled carbon nanotubes (SWCNTs) on a newly developed silica catalyst, we performed this combined experimental and theoretical study. In situ transmission electron microscopy (TEM) observations revealed that the active catalyst for the SWCNT growth is solid and amorphous SiO_x nanoparticles (NPs), suggesting a vapor−solid−solid growth mechanism. From in situ TEM and chemical vapor deposition growth experiments, we found that oxygen plays a crucial role in SWCNT growth in addition to the well-known catalyst size effect. Density functional theory calculations showed that oxygen atoms can enhance the capture of $-CH_x$ and consequently facilitate the growth of SWCNTs on oxygen-containing SiO_x NPs.

Structure-controlled growth of single-walled carbon nanotubes (SWCNTs) is one of the biggest challenges in carbon nanotube (CNT) research,[1] and it is hindered by an incomplete understanding of the growth mechanism.[2] Nanoparticles (NPs) of iron-group metals are traditional catalysts for CNT growth, where the catalyst NPs can be either liquid or solid, depending on the growth temperature, melting point, and size of the catalysts.[3] Recent studies have shown that many other metals,[4] semiconductors,[5] oxides,[6] and carbon species[7] can also grow SWCNTs, but the nature of these catalysts and the growth mechanism of SWCNTs are not well understood. Significantly, Steiner et al.[6f] elegantly demonstrated that solid ZrO_2 NPs are active catalysts that are neither reduced to Zr nor carbonized into ZrC during the whole CNT growth process. Furthermore, they hypothesized that oxygen-deficient zirconium oxide may be more active than stoichiometric zirconia.[6f] In contrast, for the growth of CNTs from silica-based catalysts,[6b−e] inconsistent conclusions about the nature of the catalyst (silica or SiC) and the CNT growth mechanism were drawn.[6d,e] Since bulk ZrO_2 has a very high melting point of 2710 °C, which is much higher than that of bulk SiO_2 (1722 °C for cristobalite, 1713 °C for vitreous SiO_2),[8] and ZrO_2 is much more difficult to reduce than SiO_2,[6f,9] the question of whether the silica catalyst is molten[6d] and Si or SiC is formed during CNT growth is still debatable. Another intriguing question concerning SWCNT growth from many new catalysts is whether all substances with a suitable particle size (e.g., <5 nm) can grow SWCNTs regardless of their chemical composition.

Here we report both experimental and theoretical studies aimed at understanding the growth mechanism of SWCNTs using silica catalysts. In situ transmission electron microscopy (TEM) studies have revealed that the active catalyst during the SWCNT growth[6b,c] is solid and amorphous SiO_x NPs, suggesting a vapor−solid−solid (VSS) growth mechanism. Comparative studies using SiO_x and Si NPs for in situ TEM and chemical vapor deposition (CVD) growth of SWCNTs have shown that having only a suitable catalyst particle size is far from sufficient and that the chemical composition of the catalyst is also of vital importance for SWCNT growth. Density functional theory (DFT) calculations have revealed that the presence of oxygen can enhance the adsorption of hydrocarbons on SiO_x NPs, thus facilitating SWCNT growth.

We conducted in situ TEM studies to monitor SWCNT growth and study the nature of the catalyst. The experiments were begun by filling SiO_x NPs (3−30 nm) into multiwalled CNTs (MWCNTs) by decomposing SiH_4 at 500 °C [see the Supporting Information (SI) and Figures S1−S3 for details]. We denote these NPs as SiO_x, since small NPs often do not follow the stoichiometry of the bulk material because of the high percentage of surface atoms. Next, a SiO_x-filled MWCNT was manipulated with a transmission electron microscope/scanning tunneling microscope holder (NanoFactory) and connected with two Au electrodes (Figure S4). When a desired current was passed through the MWCNT, Joule heating led to a local high temperature, and thus, the MWCNT served as a nanotubular furnace. The temperature of this nanofurnace could be tuned by varying the current passed. Carbon atoms generated from the MWCNT by electron-beam-induced injection[10] and thermal diffusion served as a carbon source for the nucleation and growth of SWCNTs from the loaded SiO_x NPs.

Figure 1a shows an amorphous SiO_x NP (~7 nm diameter) inside an MWCNT. Such as-loaded SiO_x NPs were free from any carbon coating before the in situ TEM experiment, as can be seen from Figure S1. When the current density passing through the MWCNT reached $\sim 2 \times 10^6$ A/cm^2 (the current was 12 μA and the CNT diameter 27 nm), a graphitic layer first appeared on the SiO_x NP surface. After the sample was continuously heated for 2 min, a

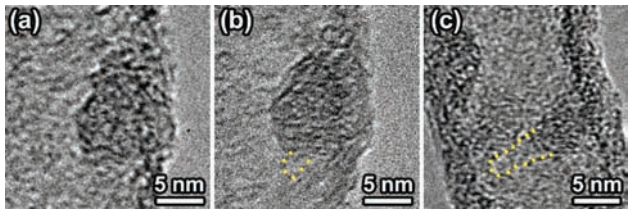

Figure 1. In situ TEM observations of the growth of SWCNTs from SiO_x NPs (also see Figures S5 and S6): (a) an original SiO_x NP; (b) the same SiO_x NP with nucleation of an SWCNT after continuous heating for 2 min; (c) an SWCNT grown from a small SiO_x NP.

[†] Chinese Academy of Sciences.
[‡] The University of Queensland.
[§] These authors contributed equally.

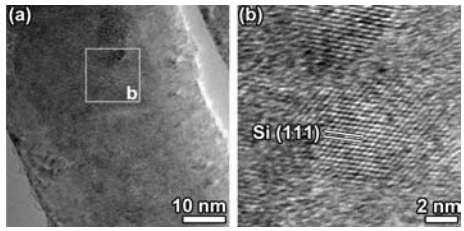

Figure 2. (a) TEM and (b) high-resolution TEM images of the Si NPs formed by in situ reduction of SiO_x NPs.

carbon cap (indicated by the yellow dotted line in Figure 1b) protruded from this SiO_x NP, indicating the nucleation and growth of a SWCNT. Figure 1c shows a grown SWCNT on another SiO_x NP with a size of ~3.7 nm, where the SWCNT stopped growing when its length reached ~8 nm because of space limitations. Comparative studies using MWCNTs without SiO_x NP loading showed no CNT formation (Figure S7), confirming that the filled SiO_x NPs served as the active catalyst for CNT growth in the in situ TEM experiments. It is important to note that during the whole growth process, the SiO_x NPs remained in an amorphous and solid state, and their shape did not substantially change. Therefore, we believe that a VSS mechanism is operative for the growth of SWCNTs on SiO_x NPs, similar to that proposed for ZrO_2-[6f] and diamond-grown SWCNTs.[7b] The solid nature and structural stability of the SiO_x catalyst should be an advantage for the growth of SWCNTs with a defined structure, as the structural fluctuation of catalysts is unfavorable for the controlled growth of SWCNTs.[11]

We also found that some SiO_x NPs were not active for SWCNT growth, and these NPs were chosen for reduction studies. When the current density was increased to ~10^7 A/cm^2 (the current was 200 μA and the CNT diameter 50 nm), SiO_x NPs were reduced to Si NPs, as validated by the lattice corresponding to Si (111) in Figure 2. The reduction temperature of SiO_x NPs has been estimated as 1100−1200 °C according to reported in situ heating experiments.[9] In contrast to the above observations for SiO_x NPs, no graphitic layers, carbon caps, or CNTs were found on the Si NPs, despite a small size of ~5 nm (Figure 2b). This result reveals the important fact that Si NPs cannot catalyze the growth of SWCNTs under similar conditions, suggesting that the chemical composition of the catalyst is of critical importance for CNT growth in addition to the well-known catalyst size effect.

To confirm the influence of the chemical composition of the catalyst on SWCNT growth, we attempted CVD growth of SWCNTs from SiO_x and Si NPs. The growth procedure was similar to that in our previous reports on the metal-catalyst-free growth of SWCNTs.[6b,c] In brief, a thin SiO_x or Si film was sputtered onto a Si or Si/SiO_2 wafer, which served as a substrate. After pretreatment under different conditions, the substrate was subjected to CH_4 CVD at 900 °C (see the SI and Figures S8−S14). Figure 3a is an atomic force microscopy (AFM) image of a Si/SiO_2 wafer with a 30 nm thick SiO_x film deposited after H_2 pretreatment, showing the formation of SiO_x NPs with an average diameter of 1.9 nm. AFM (Figure 3b) and scanning electron microscopy (SEM) images (Figure S10) showed the growth of dense SWCNTs from SiO_x NPs (Figure S11). Raman analysis revealed that these SiO_x NPs were not in a crystalline state (Figure S12), consistent with the in situ TEM observations. Because the CVD temperature was similar to or lower than the temperature in the in situ TEM experiments,[9] we believe that the SiO_x NPs also remained solid in the CVD process. In sharp contrast, when substrates with either a 30 or 5 nm thick deposited Si film were used in the same CVD process, our extensive AFM (Figure 3c,d) and SEM (Figure S13) examinations confirmed that no CNTs were formed (only Si NPs were seen). AFM height analysis showed that the sizes of these NPs were in the ranges 2−30 nm (lower panel in Figure 3c) and 0.6−3.5 nm (lower panel in Figure 3d), respectively. Moreover, these Si NPs were free of a carbon coating, since no D-band or G-band Raman signals were detected (Figure S14). We also conducted CVD experiments by varying the growth temperature and gas flow rate on the deposited Si film, but no SWCNTs were found over a reasonably broad range of process parameters. These results are consistent with the in situ TEM observations and unambiguously suggest that a suitable size of catalyst NPs is not sufficient and that the presence of oxygen (i.e., the composition of the catalyst NPs) plays a critical role in the nucleation and growth of SWCNTs from SiO_x NPs.

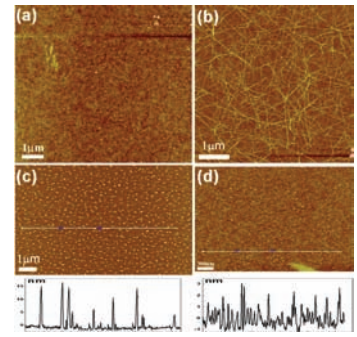

Figure 3. CVD growth of SWCNTs from deposited SiO_x and Si films. (a) AFM image of a 30-nm-thick deposited SiO_x film after H_2 pretreatment before CH_4 exposure, showing the formation of SiO_x NPs with an average size of 1.9 nm. (b) AFM image of SWCNTs grown from (a). (c, d) AFM images of (c) 30 and (d) 5 nm thick deposited Si films after CVD (upper panels) and the corresponding height analyses along the white lines (lower panels).

To confirm the role of oxygen in the catalyst for the growth of SWCNTs, we performed CVD growth experiments with different catalyst pretreatments. As presented in Figure S15, high-temperature reduction (1000 °C for 10 min; Figure S15b) reduced the efficiency of SiO_x, while high-temperature oxidation (1100 °C for 30 min; Figure S15c,d) activated Si for the growth of SWCNTs. Ex situ X-ray photoelectron spectroscopy (XPS) analysis revealed the oxidation of Si to silica after the above oxidation (Figure S16). These results confirmed a significant role of oxygen for SWCNT growth from the SiO_x catalyst, in agreement with the in situ TEM observations.

It is known that the adsorption of a carbon source on the catalyst surface is a prerequisite step toward the growth of SWCNTs on any catalyst.[2] Since the major difference between SiO_x and Si is the existence of oxygen in the former, we used DFT calculations to study the effect of oxygen on the adsorption of carbon species on Si and an oxygen-modified Si surface in order to understand how oxygen affects the growth of SWCNTs (see the SI for the calculation method).

Figures 4 and 5 show the optimized geometries of clean and oxygen-modified Si(111) surfaces, respectively, on which $-CH_x$ (x = 0, 1, 2, 3, 4) has been adsorbed. For clarity, only the top layer of Si atoms is shown as a ball-and-stick model, while the others are shown as lines. The values given are the calculated adsorption energies, with negative values indicating that such adsorption is preferable. Comparisons of these adsorption energies show that oxygen-modified surface possesses more negative adsorption energies than the clean Si(111) surface for all of the $-CH_x$ species, revealing that the existence of oxygen can enhance the capture of $-CH_x$. Notably, a positive value of 0.21 eV was obtained for adsorption of $-CH_4$ (the initial carbon species when methane

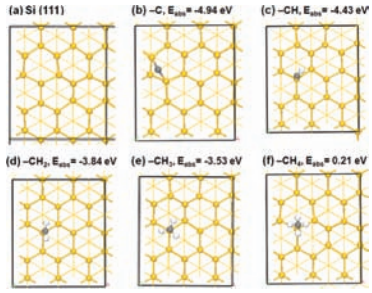

Figure 4. Optimized geometries of $-CH_x$ adsorbed on a clean Si(111) surface. Si, C, and H are indicated as yellow, gray, and white spheres, respectively. The numerical values shown are the calculated adsorption energies in eV.

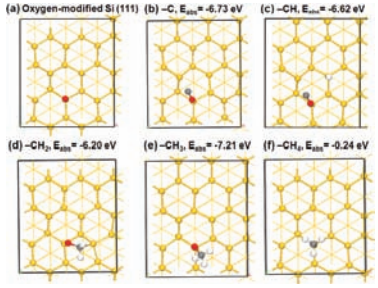

Figure 5. Optimized geometries of $-CH_x$ adsorbed on an oxygen-modified Si(111) surface. Si, O, C, and H are indicated as yellow, red, gray, and white spheres, respectively. The numerical values shown are calculated adsorption energies in eV.

is used as the carbon source) on Si(111) (Figure 4f), suggesting such adsorption is not stable. In contrast, the oxygen-modified Si(111) shows a negative adsorption energy of −0.24 eV for $-CH_4$, which can be attributed to the improved adsorption ability induced by the oxygen via hydrogen bonding between $-CH_4$ and O with a H−O distance of 1.69 Å (Figure 5f and Figure S17). The stronger adsorption of $-CH_x$ on the SiO_x surface than on clean Si(111) can provide more opportunities for C−C coupling and SWCNT nucleation. In short, relative to a Si substrate, a SiO_x surface shows much higher adsorption ability for $-CH_x$ (especially $-CH_4$), and therefore, SiO_x is superior to Si in capturing $-CH_x$ species. Notably, although Si can stably absorb −C, no SWCNTs were grown on Si NPs in our in situ TEM experiments (the main carbon species in this case was the electron-beam-injected carbon atoms);[10] this indicates that oxygen may also play an important role in promoting the formation of graphitic carbon structures, consistent with those reported by Steiner et al.[6f] and Rummeli et al.[12] However, it should be noted that Steiner et al. proposed that the presence of defects due to the extraction of oxygen play a role in the catalytic activity of ZrO_2 NPs for CNT growth.[6f] In addition, besides the adsorption of the carbon source on the catalyst surface, the growth of SWCNTs also strongly depends on the subsequent carbon source dissociation, carbon species diffusion, and SWCNT nucleation and lengthening. Therefore, it is not clear yet whether continuously increasing the oxygen content in SiO_x should ultimately favor SWCNT growth.

In conclusion, through in situ TEM and CVD growth experiments, we have studied the nature of the catalyst and the growth mechanism of SWCNTs from SiO_x NPs. We have found that SiO_x NPs are amorphous and remain in a solid state during the growth of SWCNTs. Therefore, we propose that SWCNTs are grown from SiO_x NPs following a VSS mechanism. Furthermore, comparative studies have shown that Si NPs with a similar size are inactive toward SWCNT growth, indicating that oxygen plays a critical role in the growth of the SWCNTs. These results reveal the fact that the chemical composition of the catalyst is another crucial factor for SWCNT growth in addition to the well-known catalyst size effect. DFT calculations have indicated that oxygen atoms can improve the capture of $-CH_x$ and consequently facilitate the growth of SWCNTs on SiO_x NPs. These findings highlight the importance of oxygen in the growth of SWCNTs using SiO_x catalysts and may guide the design and exploration of efficient catalysts for the controlled synthesis of SWCNTs.

Acknowledgment. We thank Prof. Dmitri Golberg for EELS mapping, Mr. Shisheng Li for film deposition, and Dr. Gang Liu for XPS analysis. B.L. acknowledges the Innovation Fund for Graduate Students of IMR, CAS (09N2A111A1). C.S. thanks the Queensland Government and UQ for financial support via a Smart Future Fellowship and a UQ ECR Grant. This work was supported by the MOST of China (2011CB932601 and 2008DFA51400), the NSFC (50921004, 50702063, and 50672103), CAS (KJCX2-YW-M01), and the Supercomputing Center, CNIC, CAS.

Supporting Information Available: Experimental and theoretical calculation details and some additional TEM, EELS, XPS, AFM, SEM, and Raman characterizations. This material is available free of charge via the Internet at http://pubs.acs.org.

References

(1) (a) Smalley, R. E.; Li, Y. B.; Moore, V. C.; Price, B. K.; Colorado, R.; Schmidt, H. K.; Hauge, R. H.; Barron, A. R.; Tour, J. M. *J. Am. Chem. Soc.* **2006**, *128*, 15824. (b) Ishigami, N.; Ago, H.; Imamoto, K.; Tsuji, M.; Iakoubovskii, K.; Minami, N. *J. Am. Chem. Soc.* **2008**, *130*, 9918.
(2) Mora, E.; Pigos, J. M.; Ding, F.; Yakobson, B. I.; Harutyunyan, A. R. *J. Am. Chem. Soc.* **2008**, *130*, 11840.
(3) Wirth, C. T.; Hofmann, S.; Robertson, J. *Diamond Relat. Mater.* **2009**, *18*, 940.
(4) (a) Bhaviripudi, S.; Mile, E.; Steiner, S. A.; Zare, A. T.; Dresselhaus, M. S.; Belcher, A. M.; Kong, J. *J. Am. Chem. Soc.* **2007**, *129*, 1516. (b) Takagi, D.; Homma, Y.; Hibino, H.; Suzuki, S.; Kobayashi, Y. *Nano Lett.* **2006**, *6*, 2642. (c) Zhou, W. W.; Han, Z. Y.; Wang, J. Y.; Zhang, Y.; Jin, Z.; Sun, X.; Zhang, Y. W.; Yan, C. H.; Li, Y. *Nano Lett.* **2006**, *6*, 2987. (d) Ritschel, M.; Leonhardt, A.; Elefant, D.; Oswald, S.; Buchner, B. *J. Phys. Chem. C* **2007**, *111*, 8414. (e) Yuan, D. N.; Ding, L.; Chu, H. B.; Feng, Y. Y.; McNicholas, T. P.; Liu, J. *Nano Lett.* **2008**, *8*, 2576. (f) Liu, B. L.; Ren, W. C.; Gao, L. B.; Li, S. S.; Liu, Q. F.; Jiang, C. B.; Cheng, H. M. *J. Phys. Chem. C* **2008**, *112*, 19231. (g) Ghorannevis, Z.; Kato, T.; Kaneko, T.; Hatakeyama, R. *J. Am. Chem. Soc.* **2010**, *132*, 9570.
(5) (a) Uchino, T.; Bourdakos, K. N.; de Groot, C. H.; Ashburn, P.; Kiziroglou, M. E.; Dilliway, G. D.; Smith, D. C. *Appl. Phys. Lett.* **2005**, *86*, 233110. (b) Takagi, D.; Hibino, H.; Suzuki, S.; Kobayashi, Y.; Homma, Y. *Nano Lett.* **2007**, *7*, 2272.
(6) (a) Liu, H.; Takagi, D.; Ohno, H.; Chiashi, S.; Chokan, T.; Homma, Y. *Appl. Phys. Express* **2008**, *1*, 014001. (b) Liu, B. L.; Ren, W. C.; Gao, L. B.; Li, S. S.; Pei, S. F.; Liu, C.; Jiang, C. B.; Cheng, H. M. *J. Am. Chem. Soc.* **2009**, *131*, 2082. (c) Liu, B. L.; Ren, W. C.; Liu, C.; Sun, C. H.; Gao, L. B.; Li, S. S.; Jiang, C. B.; Cheng, H. M. *ACS Nano* **2009**, *3*, 3421. (d) Huang, S. M.; Cai, Q. R.; Chen, J. Y.; Qian, Y.; Zhang, L. J. *J. Am. Chem. Soc.* **2009**, *131*, 2094. (e) Bachmatiuk, A.; Borrnert, F.; Grobosch, M.; Schaffel, F.; Wolff, U.; Scott, A.; Zaka, M.; Warner, J. H.; Klingeler, R.; Knupfer, M.; Buchner, B.; Rummeli, M. H. *ACS Nano* **2009**, *3*, 4098. (f) Steiner, S. A.; Baumann, T. F.; Bayer, B. C.; Blume, R.; Worsley, M. A.; MoberlyChan, W. J.; Shaw, E. L.; Schlogl, R.; Hart, A. J.; Hofmann, S.; Wardle, B. L. *J. Am. Chem. Soc.* **2009**, *131*, 12144.
(7) (a) Yao, Y. G.; Feng, C. Q.; Zhang, J.; Liu, Z. F. *Nano Lett.* **2009**, *9*, 1673. (b) Takagi, D.; Kobayashi, Y.; Homma, Y. *J. Am. Chem. Soc.* **2009**, *131*, 6922. (c) Rao, F. B.; Li, T.; Wang, Y. L. *Carbon* **2009**, *47*, 3580.
(8) *CRC Handbook of Chemistry and Physics*, 87th ed.; Lide, D. R., Ed.; Taylor and Francis: Boca Raton, FL, 2007.
(9) *In-situ Electron Microscopy at High Resolution*; Banhart, F., Ed.; World Scientific: Singapore, 2008.
(10) Rodriguez-Manzo, J. A.; Terrones, M.; Terrones, H.; Kroto, H. W.; Sun, L. T.; Banhart, F. *Nat. Nanotechnol.* **2007**, *2*, 307.
(11) Yoshida, H.; Takeda, S.; Uchiyama, T.; Kohno, H.; Homma, Y. *Nano Lett.* **2008**, *8*, 2082.
(12) Rummeli, M. H.; Kramberger, C.; Gruneis, A.; Ayala, P.; Gemming, T.; Buchner, B.; Pichler, T. *Chem. Mater.* **2007**, *19*, 4105.

JA107855Q